Malaya Journal of Matematik, Vol. 9, No. 1, 950-960, 2021

https://doi.org/10.26637/MJM0901/0170

Effect of mass transfer on unsteady three-dimensional MHD dusty Couette flow

S. Gomathi[1]*, M. Sakthi[2] and M. Shangeetha[2]

Abstract
The unsteady three-dimensional Couette flow of a viscous incompressible fluid between two porous flat plates with uniform injection and periodic suction in the presence of magnetic field and mass transfer has been investigated. Perturbation technique has been used to obtain approximate solutions for the velocity, temperature and concentration fields, skin friction, Nusselt number and Sherwood number. The velocity, temperature and concentration profiles have been plotted to study the effect of diffusion parameter, Schmidt number and other non-dimensional parameters on them. Furthermore, skin friction and Nusselt number have been tabulated for different values of the non-dimensional parameters.

Keywords
Slip flow regime, MHD, mass transfer, porous medium, Couette flow, dusty fluid.

AMS Subject Classification
54C05, 54C08, 54C10.

[1] *Department of Mathematics, P.K.R. Arts Arts College for Women, Gobi–638476, Tamil Nadu, India.*
[2] *Department of Mathematics, Kaamadhenu Arts and Science College, Sathyamangalam–638402, Tamil Nadu, India.*
***Corresponding author**: [1] gomathiselvaraj09@gmail.com
Article History: Received **14** December **2020**; Accepted **15** March **2021**

Contents

1. Introduction

Dusty Couette flows in the presence of magnetic field finds its application in many industrial process in the field of aerodynamics, nuclear cooling and geophysics. Some of their applications include investigation of underground water resources, natural gas, and mineral oils [10–15].

The unsteady hydromagnetic generalized Couette flow and heat transfer characteristics of a reactive variable viscosity incompressible electrically conducting third grade fluid in a channel with asymmetric convective cooling at the walls in the presence of uniform transverse magnetic field are studied by Chinyoka and Makinde [2]. The chemical kinetics in the flow system is assumed to be exothermic. Makinde and Chinyoka [7] investigated the unsteady generalized Couette flow and heat transfer. The authors in [9] studied the combined effects of free convective heat and mass transfer on an unsteady MHD dusty viscoelastic fluid flow. The conclusions of unsteady flow of an electrically conducting and incompressible viscoelastic liquid with simultaneous heat and mass transfer near an oscillating porous plate in slip flow regime under the presence of magnetic field is reported in [8] in which equations are solved by perturbation method. Ahmed et al. [1] reported the modeling of three-dimensional channel flow in a chemically-reacting fluid between two long vertical parallel flat plates in the presence of magnetic field, in which the magnetic parameter is found to escalate the velocity near the plate in motion. Das et al. [3] obtained a unsteady hydromagnetic Couette flow and heat transfer of a reactive viscous incompressible electrically conducting fluid between two infinitely long horizontal parallel plates in the presence of magnetic field. By Laplace transform technique, transient equations are solved the unsteady hydromagnetic Couettee flow and heat transfer of a reactive viscous incompressible fluid to obtain the velocity field and shear stresses in a unified closed form. The main aim of this work is to extend the result of Guria [6] for heat source and mass transfer function in the presence of magnetic field.

2. Flow description and governing equations

The flow under investigation is designed as an unsteady three dimensional flow of a viscous, incompressible, dusty fluid between two horizontal porous flat plates separated by a distance “d” in a slip flow regime with uniform suction at the stationary plate and periodic suction at the plate in motion. A uniform magnetic field B_0 is applied to the plate as shown in Fig.1, more details one can refer [6]. The upper plate is subjected to a constant injection $-V_0$ and the lower plate to a transverse sinusoidal time dependent suction velocity distribution of the form

$$v^* = -V_0\left[1+\varepsilon\cos\left(\frac{\pi z^*}{d^*}-ct^*\right)\right], \tag{1}$$

where $\varepsilon(\ll 1)$ represents amplitude of the suction velocity.

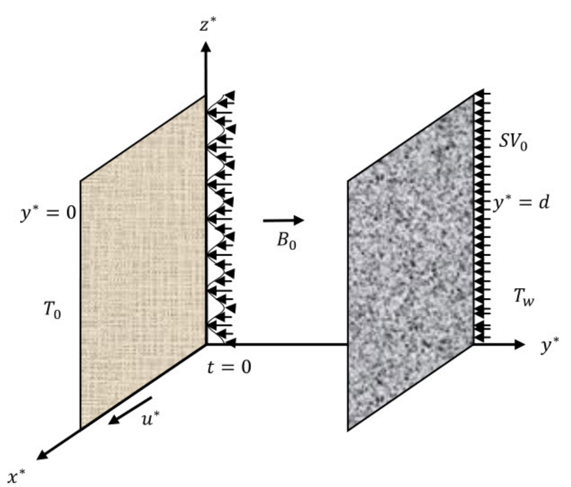

Figure 1. Couette dusty flow with constant injection and periodic suction at the porous plates.

Denoting dimensional velocity components as u^*, v^* and w^* in the directions x^*, y^* and z^* axes respectively for the fluid phase, u_p^*, v_p^* and w_p^* in the directions x^*, y^* and z^* axes respectively for the particle phase, T^* and T_p^* for the temperature of the fluid and particle phase respectively and C^* for the dilute concentration of small particles, the governing equations are mentioned as below:

For fluid phase:

$$\frac{\partial v^*}{\partial y^*}+\frac{\partial w^*}{\partial z^*}=0 \tag{2}$$

$$\begin{aligned}\frac{\partial u^*}{\partial t^*}+v^*\frac{\partial u^*}{\partial y^*}+w^*\frac{\partial u^*}{\partial z^*}&=\nu\left(\frac{\partial^2 u}{\partial y^{*2}}+\frac{\partial^2 u}{\partial z^{*2}}\right)\\&+g\beta_T(T^*-T_0)+g\beta_C(C^*-C_0)\\&-\frac{\sigma B_0^2 u^*}{\rho}+\frac{KN_0}{\rho}(u_p^*-u^*)\end{aligned} \tag{3}$$

$$\begin{aligned}\frac{\partial v^*}{\partial t^*}+v^*\frac{\partial v^*}{\partial y^*}+w^*\frac{\partial v^*}{\partial z^*}&=\nu\left(\frac{\partial^2 v}{\partial y^{*2}}+\frac{\partial^2 v}{\partial z^{*2}}\right)\\&+\frac{\partial p^*}{\partial y^*}+\frac{KN_0}{\rho}(v_p^*-v^*)\end{aligned} \tag{4}$$

$$\begin{aligned}\frac{\partial w^*}{\partial t^*}+v^*\frac{\partial w^*}{\partial z^*}&=\nu\left(\frac{\partial^2 w}{\partial y^{*2}}+\frac{\partial^2 w}{\partial z^{*2}}\right)+\frac{\partial p^*}{\partial z^*}\\&-\frac{\sigma B_0^2}{\rho}+\frac{KN_0}{\rho}(w_p^*-w^*)\end{aligned} \tag{5}$$

$$\begin{aligned}\rho C_p\left(\frac{\partial T^*}{\partial t^*}+v^*\frac{\partial T^*}{\partial y^*}+w^*\frac{\partial T^*}{\partial z^*}\right)&=K\left(\frac{\partial^2 T}{\partial y^{*2}}+\frac{\partial^2 T}{\partial z^{*2}}\right)\\&+\frac{\rho_p C_s}{\Gamma_T}(T_p^*-T^*)+Q(T^*-T_0)\end{aligned} \tag{6}$$

$$\begin{aligned}\frac{\partial C^*}{\partial t^*}+v^*\frac{\partial C^*}{\partial y^*}+w^*\frac{\partial C^*}{\partial z^*}&=D\left(\frac{\partial^2 C^*}{\partial y^{*2}}+\frac{\partial^2 C^*}{\partial z^{*2}}\right)\\&+D_T\left(\frac{\partial^2 T^*}{\partial y^{*2}}+\frac{\partial^2 T^*}{\partial z^{*2}}\right)\end{aligned} \tag{7}$$

For particle phase:

$$\frac{\partial v_p^*}{\partial y^*}+\frac{\partial w_p^*}{\partial z^*}=0 \tag{8}$$

$$\frac{\partial u_p^*}{\partial t^*}+v_p^*\frac{\partial u_p^*}{\partial y^*}+w_p^*\frac{\partial u_p^*}{\partial z^*}=\frac{K}{m_p}(u^*-u_p^*) \tag{9}$$

$$\frac{\partial v_p^*}{\partial t^*}+v_p^*\frac{\partial v_p^*}{\partial y^*}+w_p^*\frac{\partial v_p^*}{\partial z^*}=\frac{K}{m_p}(v^*-v_p^*) \tag{10}$$

$$\frac{\partial w_p^*}{\partial t^*}+v_p^*\frac{\partial w_p^*}{\partial y^*}+w_p^*\frac{\partial w_p^*}{\partial z^*}=\frac{K}{m_p}(w^*-w_p^*) \tag{11}$$

$$\frac{\partial T_p^*}{\partial t^*}+v_p^*\frac{\partial T_p^*}{\partial y^*}+w_p^*\frac{\partial T_p^*}{\partial z^*}=\frac{1}{\Gamma_p}(T^*-T_p^*), \tag{12}$$

in which all the symbols are usual meanings and are mentioned in the Appendix. Then boundary conditions are: $u^*=L_1^*\frac{\partial u^*}{\partial y^*}$; $v^*=-SV_0\left[1+\varepsilon\cos\left(\frac{\pi z^*}{d^*}-ct^*\right)\right]$; $w^*=L_1^*\frac{\partial w^*}{\partial y^*}$; $T^*=T_0+L_2^*\frac{\partial T^*}{\partial y^*}$; $C^*=C_0+L_1^*\frac{\partial C^*}{\partial y^*}$; $u_p^*=L_1^*\frac{\partial u_p^*}{\partial y^*}$; $v_p^*=-SV_0\left[1+\varepsilon\cos\left(\frac{\pi z^*}{d^*}-ct^*\right)\right]$; $w_p^*=L_1^*\frac{\partial w_p^*}{\partial y^*}$;

$$T_p^*=T_0+L_2^*\frac{\partial T^*}{\partial y^*}\quad \text{at}\quad y=0 \tag{13}$$

$u^* = U$; $v_p^* = -V_0$; $w^* = 0$; $T^* = T_1$; $C^* = C_1$; $u_p^* = U$; $v_p^* = -V_0$;

$$w_p^* = 0; \quad T_p^* = T_1 \quad \text{at} \quad y = d \tag{14}$$

where $L_1^* = \left(\frac{2-r}{r}\right)L, L_2^* = \left(\frac{2-r}{r}\right)L'$ and $L = \mu\left(\frac{\pi}{2P\rho}\right)^{1/2}$ is the mean free path and r is the Maxwell's reflection coefficient. By introducing the following non-dimensional parameters: $y = \frac{y^*}{d}$; $z = \frac{z^*}{d}$; $t = ct^*$; $p = \frac{p^*}{\rho V_0^2}$; $u = \frac{u^*}{U}$; $v = \frac{v^*}{V_0}$; $w = \frac{w^8}{V_0}$; $u_p = \frac{u_p^*}{U}$; $v_p = \frac{v_p^*}{V_0}$; $w_p = \frac{w_p^*}{V_0}$; $\theta = \frac{T^*-T_d^*}{T_0^*-T_d^*}$; $\Gamma_p = \frac{\Lambda d}{V_0}$; $\theta = \frac{T^*-T_0}{T_1-T_0}$; $\varphi = \frac{C^*-C_0}{C_1-C_0}$; $\theta_p = \frac{T_p^*-T_0}{T_1-T_0}$; Soret number $So = \frac{D_T}{D}\frac{T_1-T_0}{C_1-C_0}$; Reynolds number $Re = \frac{V_0 d}{\nu}$; Prandtl number $Pr = \frac{\mu C_p}{K}$; Schmidt number $Sc = \frac{\nu}{D}$; Hartmann number $M = \frac{\sigma B_0^2 d}{\mu}$; Mass concentration parameter $f = \frac{N_0 m}{\rho}$; Velocity slip parameter $h_1 = \frac{L_1}{d}$; Temperature slip parameter $h_2 = \frac{L_2}{d}$; Concentration slip parameter $h_3 = \frac{L_3}{d}$; Grashof number for heat transfer $Gr = \frac{g\beta_T d(T_1-T_0)}{UV_0}$; Grashof number for mass transfer $Gm = \frac{g\beta_C d(C_1-C_0)}{UV_0}$; Heat parameter $F = \frac{Qd^2}{\mu C_p}$; Frequency parameter $\lambda = \frac{cd^2}{\nu}$;

$$\text{Relaxation time parameter} \ \ \Lambda = \frac{m_p V_0}{dK}. \tag{15}$$

The governing equations (2-14) can be rewritten as follows:

$$\frac{\partial v}{\partial y} + \frac{\partial w}{\partial z} = 0 \tag{16}$$

$$\lambda\frac{\partial u}{\partial t} + Re\left(v\frac{\partial u}{\partial y} + w\frac{\partial u}{\partial z}\right) = \left(\frac{\partial^2 u}{\partial y^2} + \frac{\partial^2 u}{\partial z^2}\right) + ReGr\theta + ReGm\varphi + Mu + \frac{fRe}{\Lambda}(u_p - u) \tag{17}$$

$$\lambda\frac{\partial v}{\partial t} + Re\left(v\frac{\partial v}{\partial y} + w\frac{\partial v}{\partial z}\right) = \left(\frac{\partial^2 v}{\partial y^2} + \frac{\partial^2 v}{\partial z^2}\right) - Re\frac{\partial p}{\partial y} + \frac{fRe}{\Lambda}(v_p - v) \tag{18}$$

$$\lambda\frac{\partial w}{\partial t} + Re\left(v\frac{\partial w}{\partial y} + w\frac{\partial w}{\partial z}\right) = \left(\frac{\partial^2 w}{\partial y^2} + \frac{\partial^2 w}{\partial z^2}\right) - Re\frac{\partial p}{\partial z} + Mw + \frac{fRe}{\Lambda}(w_p - w) \tag{19}$$

$$\lambda Pr\frac{\partial \theta}{\partial t} + RePr\left(v\frac{\partial \theta}{\partial y} + w\frac{\partial \theta}{\partial z}\right) = \left(\frac{\partial^2 \theta}{\partial y^2} + \frac{\partial^2 \theta}{\partial z^2}\right) + RePrF\theta + \frac{2}{3}\frac{fRe}{\Lambda}(\theta_p - \theta) \tag{20}$$

$$\lambda Sc\frac{\partial \varphi}{\partial t} + ReSc\left(v\frac{\partial \varphi}{\partial y} + w\frac{\partial \varphi}{\partial z}\right) = \left(\frac{\partial^2 \varphi}{\partial y^2} + \frac{\partial^2 \varphi}{\partial z^2}\right) + ReScSo\left(\frac{\partial^2 \theta}{\partial y^2} + \frac{\partial^2 \theta}{\partial z^2}\right) \tag{21}$$

$$\frac{\partial v_p}{\partial y} + \frac{\partial w_p}{\partial z} = 0 \tag{22}$$

$$\lambda\frac{\partial u_p}{\partial t} + Re\left(v_p\frac{\partial u_p}{\partial y} + w_p\frac{\partial u_p}{\partial z}\right) = \frac{Re}{\Lambda}(u - u_p) \tag{23}$$

$$\lambda\frac{\partial v_p}{\partial t} + Re\left(v_p\frac{\partial v_p}{\partial y} + w_p\frac{\partial v_p}{\partial z}\right) = \frac{Re}{\Lambda}(v - v_p) \tag{24}$$

$$\lambda\frac{\partial w_p}{\partial t} + Re\left(v_p\frac{\partial w_p}{\partial y} + w_p\frac{\partial w_p}{\partial z}\right) = \frac{Re}{\Lambda}(w - w_p) \tag{25}$$

$$\lambda\frac{\partial \theta_p}{\partial t} + Re\left(v_p\frac{\partial \theta_p}{\partial y} + w_p\frac{\partial \theta_p}{\partial z}\right) = \frac{Re}{\Lambda}(\theta - \theta_p) \tag{26}$$

The corresponding boundary conditions are $u = h_1\frac{\partial u}{\partial y}$; $v = -S[1+\varepsilon\cos(\pi z - t)]$; $w = h_1\frac{\partial w}{\partial y}$; $\theta = h_2\frac{\partial \theta}{\partial y}$; $\varphi = 0$

$$u_p = h_1\frac{\partial u_p}{\partial y};\ v_p = -S_1[1+\varepsilon\cos(\pi z - t)];\ w_p = h_1\frac{\partial w_p}{\partial y};\ \theta_p = h_2\frac{\partial \theta_p}{\partial y} \quad \text{at} \quad y = 0 \tag{27}$$

$$u = 1;\ v = -S;\ w = 0;\ \theta = 1\ \ \varphi = 1;\ u_p = 1;\ v_p = -S;\ w_p = 0;\ \theta_p = 1 \quad \text{at} \quad y = 1 \tag{28}$$

3. Result of the problem

When the amplitude of oscillation in the suction velocity is small ($\varepsilon \ll 1$), we can take u, v, w, θ, u_p, v_p, w_p, θ_p and p in the upcoming form to solve the equations (16)-(28).

$$\begin{aligned}
u(y,z,t) &= u_0(y) + \varepsilon u_1(y,z,t) + \cdots \\
v(y,z,t) &= v_0(y) + \varepsilon v_1(y,z,t) + \cdots \\
w(y,z,t) &= w_0(y) + \varepsilon w_1(y,z,t) + \cdots \\
\theta(y,z,t) &= \theta_0(y) + \varepsilon \theta_1(y,z,t) + \cdots \\
u_p(y,z,t) &= u_{p_0}(y) + \varepsilon u_{p_1}(y,z,t) + \cdots \\
v_p(y,z,t) &= v_{p_0}(y) + \varepsilon v_{p_1}(y,z,t) + \cdots \\
w_p(y,z,t) &= w_{p_0}(y) + \varepsilon w_{p_1}(y,z,t) + \cdots \\
\theta_p(y,z,t) &= \theta_{p_0}(y) + \varepsilon \theta_{p_1}(y,z,t) + \cdots \\
p(y,z,t) &= p_0(y) + \varepsilon p_1(y,z,t) + \cdots
\end{aligned} \tag{29}$$

When $\varepsilon = 0$, the equations are attained as below:

$$v_0' = 0 \quad (30)$$

$$u_0'' - Rev_0u_0' + ReGr\theta_0 + ReGm\varphi_0 + Mu_0 + \frac{fRe}{\Lambda}(u_{p_0} - u_0) = 0 \quad (31)$$

$$p_0' = \frac{f}{\Lambda}(v_{p_0} - v_0) \quad (32)$$

$$w_0'' - Rev_0w_0' + \frac{fRe}{\Lambda}(w_{p_0} - w_0) + Mw_0 = 0 \quad (33)$$

$$\theta_0'' - RePrv_0\theta_0' + \frac{2}{3}\frac{fRe}{\Lambda}(\theta_{p_0} - \theta_0) = 0 \quad (34)$$

$$\varphi_0'' - ReScv_0\varphi_0' - ReScSo\varphi_0 = 0 \quad (35)$$

$$v_{p_0}' = 0 \quad (36)$$

$$v_0u_{p_0}' + \frac{1}{\Lambda}(u_{p_0} - u_0) = 0 \quad (37)$$

$$v_{p_0} = v_0 \quad (38)$$

$$v_{p_0}w_{p_0}' + \frac{1}{\Lambda}(w_{p_0} - w_0) = 0 \quad (39)$$

$$v_{p_0}\theta_{p_0}' + \frac{1}{\Lambda}(\theta_{p_0} - \theta_0) = 0 \quad (40)$$

Subject to the boundary conditions

$$u_0 = h_1\frac{\partial u_0}{\partial y};\ v_0 = -S;\ w_0 = h_1\frac{\partial w_0}{\partial y};\ \theta_0 = h_2\frac{\partial \theta_0}{\partial y};$$
$$\varphi_0 = h_3\frac{\partial C_0}{\partial y},;\ u_{p_0} = h_1\frac{\partial u_{p_0}}{\partial y};\ v_{p_0} = -S;$$
$$w_{p_0} = h_1\frac{\partial w_{p_0}}{\partial y};\ \theta_{p_0} = h_2\frac{\partial \theta_{p_0}}{\partial y}; \quad \text{at} \quad y = 0 \quad (41)$$

$$u_0 = 1;\ v_0 = -S;\ w_0 = 0;\ \theta_0 = 1;\ \varphi_0 = 1;$$

$$u_{p_0} = 1;\ v_{p_0} = -S;\ w_{p_0} = 0;\ \theta_{p_0} = 1;\ \text{at}\ y = 1 \quad (42)$$

The solutions for the equations (30), (32), (36) and (38) are

$$v_0 = v_{p_0} = -S \quad (43)$$

$$p_0' = 0 \quad (44)$$

Substituting equations (43)-(44) in the remaining equations and rearranging as done in Govindarajan et al. [5], we get

$$-\Lambda Su_0''' + (1 - Re\Lambda S^2)u_0'' + (ReS(1+f) + \Lambda MS)u_0' - Mu_0 = -ReGr\theta_0 + \Lambda ReGrS\theta_0' - ReGm\varphi_0 + \Lambda ReGmS\varphi_0' \quad (45)$$

$$-\Lambda Sw_0''' + (1 - Re\Lambda S^2)w_0'' + (ReS(1+f) + \Lambda MS)w_0' - Mw_0 = 0 \quad (46)$$

$$-\Lambda S\theta_0''' + (1 - RePr\Lambda S^2)\theta_0'' + \big(ReS\big(Pr + \frac{2}{3}f\big) + \Lambda SPrF\big)\theta_0' - PrF\theta_0 = 0 \quad (47)$$

$$\varphi_0'' - ReScv_0\varphi_0' - ReScSo\varphi_0 = \theta_0'' \quad (48)$$

$$-\Lambda Su_{p_0}' + u_{p_0} = u_0 \quad (49)$$

$$-\Lambda Sw_{p_0}' + w_{p_0} = w_0 \quad (50)$$

$$\Lambda S\theta_{p_0}' + \theta_{p_0} = \theta_0 \quad (51)$$

The solution to the remaining equations are:

$$w_0 = w_{p_0} = 0 \quad (52)$$

$$\theta_0 = A_1e^{J_1y} + A_2e^{J_2y} + A_3e^{J_3y} \quad (53)$$

$$\theta_{p_0} = A_4e^{J_4y} + \frac{A_1}{(1-\Lambda J_1)}e^{J_1}y + \frac{A_2}{(1-\Lambda J_2)}e^{J_2}y + \frac{A_3}{(1-\Lambda J_3)}e^{J_3}y \quad (54)$$

$$\varphi_0 = A_0e^{J_0y} + A_5 + A_6e^{J_1y} + A_7e^{J_2y} + A_8e^{J_3y} \quad (55)$$

$$u_0 = A_9e^{J_5y} + A_{10}e^{J_6y} + A_{11}e^{J_7y} + A_{12}e^{J_1y} + A_{13}e^{J_2y} + A_{14}e^{J_3y} + A_{15}e^{J_0y} + A_{16} \quad (56)$$

$$u_{p_0} = A_{17}e^{J_4y} + A_{18}e^{J_5y} + A_{19}e^{J_6y} + A_{20}e^{J_7y} + A_{21}e^{J_1y} + A_{22}e^{J_2y} + A_{23}e^{J_3y} + A_{24}e^{J_0y} + A_{25} \quad (57)$$

The unsteady state equations of first order are:

$$\frac{\partial v_1}{\partial y} + \frac{\partial w_1}{\partial z} = 0 \quad (58)$$

$$\lambda\frac{\partial u_1}{\partial t} + Re\left(-S\frac{\partial u_1}{\partial y} + v_1\frac{\partial u_0}{\partial y}\right) = \left(\frac{\partial^2 u_1}{\partial y^2} + \frac{\partial^2 u_1}{\partial z^2}\right) + ReGr\theta_1 + ReGr\varphi_1 - Mu_1 + \frac{fRe}{\Lambda}(u_{p_1} - u_1) \quad (59)$$

$$\lambda\frac{\partial v_1}{\partial t} + Re\left(-S\frac{\partial v_1}{\partial y}\right) = \left(\frac{\partial^2 v_1}{\partial y^2} + \frac{\partial^2 v_1}{\partial z^2}\right) - Re\frac{\partial p_1}{\partial y} + \frac{fRe}{\Lambda}(v_{p_1} - v_1) \quad (60)$$

$$\lambda\frac{\partial w_1}{\partial t} + Re\left(-S\frac{\partial w_1}{\partial y}\right) = \left(\frac{\partial^2 w_1}{\partial y^2} + \frac{\partial^2 w_1}{\partial z^2}\right) - Re\frac{\partial p_1}{\partial z} - Mw_1 + \frac{fRe}{\Lambda}(w_{p_1} - w_1) \quad (61)$$

$$\lambda Pr\frac{\partial \theta_1}{\partial t} + RePr\left(-S\frac{\partial \theta_1}{\partial y} + v_1\frac{\partial \theta_0}{\partial y}\right) = \left(\frac{\partial^2 \theta_1}{\partial y^2} + \frac{\partial^2 \theta_1}{\partial z^2}\right) - PrF\theta + \frac{2}{3}\frac{fRe}{\Lambda}(\theta_{p_1} - \theta_1) \quad (62)$$

$$\lambda Sc\frac{\partial \varphi_1}{\partial t} + ReSc\left(-S\frac{\partial \varphi_1}{\partial y} + v_1\frac{\partial \varphi_0}{\partial y}\right) = \left(\frac{\partial^2 \varphi_1}{\partial y^2} + \frac{\partial^2 \varphi_1}{\partial z^2}\right) + ReScSo\left(\frac{\partial^2 \theta_1}{\partial y^2} + \frac{\partial^2 \theta_1}{\partial z^2}\right) \quad (63)$$

$$\frac{\partial v_{p_1}}{\partial y} + \frac{\partial w_{p_1}}{\partial z} = 0 \quad (64)$$

$$\lambda\frac{\partial u_{p_1}}{\partial t} + Re\left(-S\frac{\partial u_{p_1}}{\partial y} + v_{p_1}\frac{\partial u_{p_0}}{\partial y}\right) = \frac{Re}{\Lambda}(u_1 - u_{p_1}) \quad (65)$$

$$\lambda\frac{\partial v_{p_1}}{\partial t} + Re\left(-S\frac{\partial v_{p_1}}{\partial y}\right) = \frac{Re}{\Lambda}(v_1 - v_{p_1}) \quad (66)$$

$$\lambda \frac{\partial w_{p_1}}{\partial t} + Re\left(-S\frac{\partial w_{p_1}}{\partial y}\right) = \frac{Re}{\Lambda}(w_1 - w_{p_1}) \tag{67}$$

$$\lambda \frac{\partial \theta_{p_1}}{\partial t} + Re\left(-S\frac{\partial \theta_{p_1}}{\partial y} + v_{p_1}\frac{\partial \theta_{p_0}}{\partial y}\right) = \frac{Re}{\Lambda}(\theta_1 - \theta_{p_1}) \tag{68}$$

The boundary conditions become

$$u_1 = h_1\frac{\partial u_1}{\partial y};\ v_1 = -S(\cos(\pi z - t));\ w_1 = h_1\frac{\partial w_1}{\partial y};$$
$$\theta_1 = h_2\frac{\partial \theta_1}{\partial y};\ \varphi_1 = h_3\frac{\partial \varphi_1}{\partial y};$$
$$u_{p_1} = h_1\frac{\partial u_{p_1}}{\partial y};\ v_{p_1} = -S(\cos(\pi z - t));$$
$$w_{p_1} = h_1\frac{\partial w_{p_1}}{\partial y};\theta_{p_1} = h_2\frac{\partial \theta_{p_1}}{\partial y};\ \text{at}\ y=0 \tag{69}$$

$$u_1 = v_1 = w_1 = \theta_1 = \varphi_1 = u_{p_1} = v_{p_1} = w_{p_1} = \theta_{p_1} = 0 \tag{70}$$

In order to solve these partial differential equations u_1, v_1, w_1, θ_1, φ_1, u_{p_1}, v_{p_1}, w_{p_1}, θ_{p_1}, and p_1 are given to be of the upcoming form:

$$\begin{aligned}
u_1(y,z,t) &= u_{11}(y)e^{i(\pi z - t)}\\
v_1(y,z,t) &= v_{11}(y)e^{i(\pi z - t)}\\
w_1(y,z,t) &= \frac{i}{\pi}v'_{11}(y)e^{i(\pi z - t)}\\
\theta_1(y,z,t) &= \theta_{11}(y)e^{i(\pi z - t)}\\
u_{p_1}(y,z,t) &= u_{p_{11}}(y)e^{i(\pi z - t)}\\
v_{p_1}(y,z,t) &= v_{p_{11}}(y)e^{i(\pi z - t)}\\
w_{p_1}(y,z,t) &= \frac{i}{\pi}v'_{p_{11}}(y)e^{i(\pi z - t)}\\
\theta_{p_1}(y,z,t) &= \theta_{p_{11}}(y)e^{i(\pi z - t)}\\
p_1(y,z,t) &= p_{11}(y)e^{i(\pi z - t)}
\end{aligned} \tag{71}$$

Now using (71) in equations (58)-(70) and rearranging as before, we get

$$u''_{11} + ReSu'_{11} + (-\pi^2 + i\lambda - M)u_{11} + \frac{fRe}{\Lambda}(u_{p_{11}} - u_{11}) = -ReGr\theta_{11} - ReGm\varphi_{11} + Rev_{11}u'_0 \tag{72}$$

$$v''_{11} + ReSv'_{11} + (-\pi^2 + i\lambda)v_{11} + \frac{fRe}{\Lambda}(v_{p_{11}} - v_{11}) = Rep'_{11} \tag{73}$$

$$v''_{11} + ReSv'_{11} + (-\pi^2 + i\lambda - M)v'_{11} + \frac{fRe}{\Lambda}(v'_{p_{11}} - v'_{11}) = \pi^2 Rep'_{11} \tag{74}$$

$$\theta''_{11} + RePrS\theta'_{11} + (-\pi^2 + i\lambda Pr - PrF)\theta'_{11} + \frac{2}{3}\frac{fRe}{\Lambda}(\theta'_{p_{11}} - \theta'_{11}) = RePrv_{11}\theta'_0 \tag{75}$$

$$\varphi''_{11} + ReScS\varphi'_{11} + (-\pi^2 + i\lambda Sc)\varphi_{11} = ReScv_{11}\varphi'_0 + ReScSo(\theta''_{11} - \pi^2\theta_{11}) \tag{76}$$

$$-\Lambda u'_{p_{11}} + \left(1 - \frac{i\lambda\Lambda}{Re}\right)u_{p_{11}} = u_{11} - \Lambda v_{11}u'_{p_0} \tag{77}$$

$$-\Lambda v'_{p_{11}} + \left(1 - \frac{i\lambda\Lambda}{Re}\right)v_{p_{11}} = v_{11} \tag{78}$$

$$-\Lambda v''_{p_{11}} + \left(1 - \frac{i\lambda\Lambda}{Re}\right)v'_{p_{11}} = v'_{11} \tag{79}$$

$$-\Lambda \theta'_{p_{11}} + \left(1 - \frac{i\lambda\Lambda}{Re}\right)\theta_{p_{11}} = \theta_{11} - \Lambda v_{p_{11}}\theta'_{p_0} \tag{80}$$

$$u_{11} = h_1\frac{\partial u_{11}}{\partial y};\ v_{11} = -S;\ w_{11} = h_1\frac{\partial w_{11}}{\partial y};\ \theta_{11} = h_2\frac{\partial \theta_{11}}{\partial y};$$
$$\varphi_{11} = h_3\frac{\partial \varphi_{11}}{\partial y};u_{p_{11}} = h_1\frac{\partial u_{p_{11}}}{\partial y};\ v_{p_{11}} = -S;$$
$$;w_{p_{11}} = h_1\frac{\partial w_{p_{11}}}{\partial y};\ \theta_{p_{11}} = h_2\frac{\partial \theta_{p_{11}}}{\partial y};\ \text{at}\ y=0 \tag{81}$$

$$u_{11} = v_{11} = w_{11} = \theta_{11} = u_{p_{11}} = v_{p_{11}} = w_{p_{11}} = \theta_{p_{11}} = 0\ \text{at}\ y=1 \tag{82}$$

The result of the equations (72)-(80) with respect to boundary conditions (81)-(82) are

$$v_{11} = B_1e^{J_8y} + B_2e^{J_9y} + B_3e^{J_{10}y} + B_4e^{J_{11}y} + B_5e^{J_{12}y} + B_6e^{J_{13}y} \tag{83}$$

$$v_{p_{11}} = B_7e^{J_{14}y} + B_8e^{J_8y} + B_9e^{J_9y} + B_{10}e^{J_{10}y} + B_{11}e^{J_{11}y} + B_{12}e^{J_{12}y} + B_{13}e^{J_{13}y} \tag{84}$$

$$w_{11} = \frac{i}{\pi}[B_1J_8e^{J_8y} + B_2J_9e^{J_9y} + B_3J_{10}e^{J_{10}y} + B_4J_{11}e^{J_{11}y} + B_5e^{J_{12}y} + B_6J_{13}e^{J_{13}y}] \tag{85}$$

$$w_{p_{11}} = \frac{i}{\pi}(B_7J_{14}e^{J_{14}y} + B_8J_8e^{J_8y} + B_9J_9e^{J_9y} + B_{10}J_{10}e^{J_{10}y} + B_{11}J_{11}e^{J_{11}y} + B_{12}J_{12}e^{J_{12}y} + B_{13}J_{13}e^{J_{13}y}) \tag{86}$$

$$\begin{aligned}
\theta_{11} = {}& C_1e^{J_{15}y} + C_2e^{J_{16}y} + C_3e^{J_{17}y} + (C_4e^{J_8y} + C_5e^{J_9y} + C_6e^{J_{10}y} + C_7e^{J_{11}y} + C_8e^{J_{12}y} + C_9e^{J_{13}y}\\
&+ C_{10}e^{J_{14}y})e^{J_1y} + (C_{11}e^{J_8y} + C_{12}e^{J_9y} + C_{13}e^{J_{10}y} + C_{14}e^{J_{11}y} + C_{15}e^{J_{12}y} + C_{16}e^{J_{13}y} + C_{17}e^{J_{14}y})e^{J_2y}\\
&+ (C_{18}e^{J_8y} + C_{19}e^{J_9y} + C_{20}e^{J_{10}y} + C_{21}e^{J_{11}y} + C_{22}e^{J_{12}y} + C_{23}e^{J_{13}y} + C_{24}e^{J_{14}y})e^{J_3y} + (C_{25}e^{J_8y} +\\
&C_{26}e^{J_9y} + C_{27}e^{J_{10}y} + C_{28}e^{J_{11}y} + C_{29}e^{J_{12}y} + C_{30}e^{J_{13}y} + C_{31}e^{J_{14}y})e^{J_4y}
\end{aligned} \tag{87}$$

$$\theta_{p_{11}} = C_{32}e^{J_{14}y} + C_{33}e^{J_{15}y} + C_{34}e^{J_{16}y} + C_{35}e^{J_{17}y} + (C_{36}e^{J_8y} + C_{37}e^{J_9y} + C_{38}e^{J_{10}y} + C_{39}e^{J_{11}y} + C_{40}e^{J_{12}y} + C_{41}e^{J_{13}y} + C_{42}e^{J_{14}y})e^{J_1y} + (C_{43}e^{J_8y} + C_{44}e^{J_9y} + C_{45}e^{J_{10}y} + C_{46}e^{J_{11}y} + C_{47}e^{J_{12}y} + C_{48}e^{J_{13}y} + C_{49}e^{J_{14}y})e^{J_{12}y} + (C_{50}e^{J_8y} + C_{51}e^{J_9y} + C_{52}e^{J_{10}y} + C_{53}e^{J_{11}y} + C_{54}e^{J_{12}y} + C_{55}e^{J_{13}y} + C_{56}e^{J_{14}y})e^{J_{13}y} + (C_{57}e^{J_8y} + C_{58}e^{J_9y} + C_{59}e^{J_{10}y} + C_{60}e^{J_{11}y} + C_{61}e^{J_{12}y} + C_{62}e^{J_{13}y} + C_{63}e^{J_{14}y})e^{J_4y} \tag{88}$$

$$\varphi_{p_{11}} = E_1e^{J_{15}y} + E_2e^{J_{16}y} + E_3e^{J_{15}y} + E_4e^{J_{16}y} + E_5e^{J_{17}y} + (E_6e^{J_8y} + E_7e^{J_9y} + E_8e^{J_{10}y} + E_9e^{J_{11}y} + E_{10}e^{J_{12}y} + E_{11}e^{J_{13}y} + E_{12}e^{J_{14}y})e^{J_1y} + (E_{13}e^{J_8y} + E_{14}e^{J_9y} + E_{15}e^{J_{10}y} + E_{16}e^{J_{11}y} + E_{17}e^{J_{12}y} + E_{18}e^{J_{13}y} + E_{19}e^{J_{14}y})e^{J_2y} + (E_{20}e^{J_8y} + E_{21}e^{J_9y} + E_{22}e^{J_{10}y} + E_{23}e^{J_{11}y} + E_{24}e^{J_{12}y} + E_{25}e^{J_{13}y} + E_{26}e^{J_{14}y})e^{J_3y} + (E_{27}e^{J_8y} + E_{28}e^{J_9y} + E_{29}e^{J_{10}y} + E_{30}e^{J_{11}y} + E_{31}e^{J_{12}y} + E_{32}e^{J_{13}y} + E_{33}e^{J_{14}y})e^{J_4y} + (E_{34}e^{J_8y} + E_{35}e^{J_9y} + E_{36}e^{J_{10}y} + E_{37}e^{J_{11}y} + E_{38}e^{J_{12}y} + E_{39}e^{J_{13}y})e^{J_0y} \tag{89}$$

$$u_{11} = D_1e^{J_{18}y} + D_2e^{J_{19}y} + D_3e^{J_{20}y} + D_4e^{J_{15}y} + D_5e^{J_{16}y} + D_6e^{J_{17}y} + (D_7e^{J_8y} + D_8e^{J_9y} + D_9e^{J_{10}y} + D_{10}e^{J_{11}y} + D_{11}e^{J_{12}y} + D_{12}e^{J_{13}y} + D_{13}e^{J_{14}y})e^{J_1y} + (D_{14}e^{J_8y} + D_{15}e^{J_9y} + D_{16}e^{J_{10}y} + D_{17}e^{J_{11}y} + D_{18}e^{J_{12}y} + D_{19}e^{J_{13}y} + D_{20}e^{J_{14}y})e^{J_2y} + (D_{21}e^{J_8y} + D_{22}e^{J_9y} + D_{23}e^{J_{10}y} + D_{24}e^{J_{11}y} + D_{25}e^{J_{12}y} + D_{26}e^{J_{13}y} + D_{27}e^{J_{14}y})e^{J_3y} + (D_{28}e^{J_8y} + D_{29}e^{J_9y} + D_{30}e^{J_{10}y} + D_{31}e^{J_{11}y} + D_{32}e^{J_{12}y} + D_{33}e^{J_{13}y} + D_{34}e^{J_{14}y})e^{J_4y} + (D_{35}e^{J_8y} + D_{36}e^{J_9y} + D_{37}e^{J_{10}y} + D_{38}e^{J_{11}y} + D_{39}e^{J_{12}y} + D_{40}e^{J_{13}y} + D_{41}e^{J_{14}y})e^{J_5y} + (D_{42}e^{J_8y} + D_{43}e^{J_9y} + D_{44}e^{J_{10}y} + D_{45}e^{J_{11}y} + D_{46}e^{J_{12}y} + D_{47}e^{J_{13}y} + D_{48}e^{J_{14}y})e^{J_6y} + (D_{49}e^{J_8y} + D_{50}e^{J_9y} + D_{51}e^{J_{10}y} + D_{52}e^{J_{11}y} + D_{53}e^{J_{12}y} + D_{54}e^{J_{13}y} + D_{55}e^{J_{14}y})e^{J_7y} + (H_1e^{J_8y} + H_2e^{J_9y} + H_3e^{J_{10}y} + H_4e^{J_{11}y} + H_5e^{J_{12}y} + H_6e^{J_{13}y} + H_7e^{J_{14}y})e^{J_0y} + H_8e^{J_{21}y} + H_9e^{J_{22}y} \tag{90}$$

$$u_{p_{11}} = D_{56}e^{J_{14}y} + D_{57}e^{J_{18}y} + D_{58}e^{J_{19}y} + D_{59}e^{J_{20}y} + D_{60}e^{J_{15}y} + D_{61}e^{J_{16}y} + D_{62}e^{J_{17}y} + (D_{63}e^{J_8y} + D_{64}e^{J_9y} + D_{65}e^{J_{10}y} + D_{66}e^{J_{11}y} + D_{67}e^{J_{12}y} + D_{68}e^{J_{13}y} + D_{69}e^{J_{14}y})e^{J_1y} + (D_{70}e^{J_8y} + D_{71}e^{J_9y} + D_{72}e^{J_{10}y} + D_{73}e^{J_{11}y} + D_{74}e^{J_{12}y} + D_{75}e^{J_{13}y} + D_{76}e^{J_{14}y})e^{J_2y} + (D_{77}e^{J_8y} + D_{78}e^{J_9y} + D_{79}e^{J_{10}y} + D_{80}e^{J_{11}y} + D_{81}e^{J_{12}y} + D_{82}e^{J_{13}y} + D_{83}e^{J_{14}y})e^{J_3y} + (D_{84}e^{J_8y} + D_{85}e^{J_9y} + D_{86}e^{J_{10}y} + D_{87}e^{J_{11}y} + D_{88}e^{J_{12}y} + D_{89}e^{J_{13}y} + D_{90}e^{J_{14}y})e^{J_4y} + (D_{91}e^{J_8y} + D_{92}e^{J_9y} + D_{93}e^{J_{10}y} + D_{94}e^{J_{11}y} + D_{95}e^{J_{12}y} + D_{96}e^{J_{13}y} + D_{97}e^{J_{14}y})e^{J_5y} + (D_{98}e^{J_8y} + D_{99}e^{J_9y} + D_{100}e^{J_{10}y} + D_{101}e^{J_{11}y} + D_{102}e^{J_{12}y} + D_{103}e^{J_{13}y} + D_{104}e^{J_{14}y})e^{J_6y} + (D_{105}e^{J_8y} + D_{106}e^{J_9y} + D_{107}e^{J_{10}y} + D_{108}e^{J_{11}y} + D_{109}e^{J_{12}y} + D_{110}e^{J_{13}y} + D_{111}e^{J_{14}y})e^{J_7y} + (H_{10}e^{J_8y} + H_{11}e^{J_9y} + H_{12}e^{J_{10}y} + H_{13}e^{J_{11}y} + H_{14}e^{J_{12}y} + H_{15}e^{J_{13}y} + H_{16}e^{J_{14}y})e^{J_0y} + H_{17}e^{J_{21}y} + H_{18}e^{J_{22}y} \tag{91}$$

SKIN FRICTION

Due to the given primary flow, the skin friction at the wall is represented by:

$$\tau_x = \left(\frac{du}{dy}\right)_{y=0} = \left(\frac{du_0}{dy}\right)_{y=0} + \varepsilon\left(\frac{du_{11}}{dy}\right)_{y=0} e^{i(\phi z - t)} + \mathcal{O}(\varepsilon^2)$$

$$= \tau_{u_0} + \varepsilon Re_x \cos(\phi z - t + \phi_x) \tag{92}$$

Due to the given cross flow, the skin friction at the wall is represented by:

$$\tau_z = \left(\frac{dw}{dy}\right)_{y=0} = \left(\frac{dw_0}{dy}\right)_{y=0} + \varepsilon\left(\frac{dw_{11}}{dy}\right)_{y=0} e^{i(\phi z - t)} + \mathcal{O}(\varepsilon^2) = \varepsilon Re_z \cos(\phi z - t + \phi_z) \tag{93}$$

NUSSELT NUMBER

The rate of heat transfer is estimated by the formula $q_w = -\left(\frac{\partial T}{\partial y}\right)_{y=0}$ and can be written in non-dimensional form as Nusselt number:

$$Nu = -\left(\frac{d\theta}{dy}\right)_{y=0} = -\left(\frac{d\theta_0}{dy}\right)_{y=0} - \varepsilon\left(\frac{d\theta_{11}}{dy}\right)_{y=0} e^{i(\phi z - t)} + \mathcal{O}(\varepsilon^2) = -\theta_0'(0) + \varepsilon Re_T \cos(\phi z - t + \phi_T) \tag{94}$$

SHERWOOD NUMBER

The rate of mass transfer is estimated by the formula $m_w = -\left(\frac{\partial C}{\partial y}\right)_{y=0}$ and can be written in non-dimensional form as Sherwood number:

$$Sh = -\left(\frac{d\varphi}{dy}\right)_{y=0} = -\left(\frac{d\varphi_0}{dy}\right)_{y=0} - \varepsilon\left(\frac{d\varphi_{11}}{dy}\right)_{y=0} e^{i(\phi z - t)} + \mathcal{O}(\varepsilon^2)$$

$$= -\varphi_0'(0) + \varepsilon Re_m \cos(\phi z - t + \phi_m) \tag{95}$$

For the sake of brevity, the constants are given in Appendix.

4. Numerical Results

The velocity, temperature and concentration profiles are given in Fig.2 to Fig.11 to report the effect of different non-dimensional parameters on the profiles. Then, skin friction, Nusselt number and Sherwood number are tabulated (Table 1-4) for various values of non-dimensional parameters such as Grashof number for mass transfer (Gm), Schmidt number (Sc) and Soret number (So).

Increasing the Schmidt number (Sc) and Soret number (So) results in an increase in the particle concentration in the fluid (Fig.2-3). Increasing the Soret number results in an increase in the main flow velocity for both fluid and particle phase but it has no effect on the cross flow velocity (Fig 10-11). Alternately, increasing the Schmidt number (Sc) results in a decrease in the main flow velocity with no effect on the cross flow velocity (Fig.8).

Increase in the Reynolds number (Re) results in a rise in the amplitude of oscillations in the particle concentration (Fig 4). The particle concentration increases a little for increasing Prandtl number, but becomes constant at higher values (Fig.5). Higher values of slip mass parameter imply a larger particle concentration as can be seen in Fig.6. Increasing the Grashof number for mass transfer results in a decrease in the main flow velocity similarly as earlier observed for Grashof number for heat transfer (Fig.9). The particle concentration are found to decrease with increasing heat source parameter accompanied by a sharp change of profile as can be seen in Fig.7.

The amplitude of the shear stress and the tangent of phase shift due to main flow decreases with the increasing Schmidt number (Sc) while the amplitude of the shear stress increases with increasing Soret number (So) (Table 1). Increasing the magnitude of Grashof number for mass transfer results in an increase in magnitudes of the shear stress and the tangent of phase shift (Table 2).

Increasing the Soret number (So) results in an increase in the amplitude of Sherwood number and the tangent of phase shift (Table 3). There is no clear trend for the Sherwood number with increase in Schmidt number (Sc). The Sherwood number is found to increase with increasing mass slip parameter at lower Reynolds number and decrease with increasing mass slip parameter at higher Reynolds number (Table 4).Further, the tangent of phase shift of Sherwood number is found to generally increase with increasing mass slip parameter.

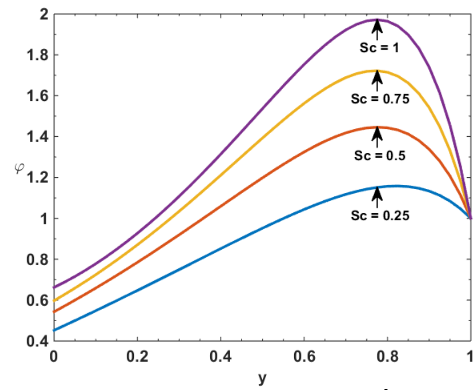

Figure 2. Particle concentration φ vs y for $\lambda = 5$, $Re = 2$, $Gr = .5$, $Gm = -.5$, $Pr = 0.71$, $So = 1.5$, $S = 1$, $F = 1$, $M = 1$, $h_1 = 0.5$, $h_2 = 0.5$, $h_3 = 0.5$, $f = 0.2$, $\Lambda = 0.2$, $z = 0.0$, $t = 0.0$, $\varepsilon = 0.05$

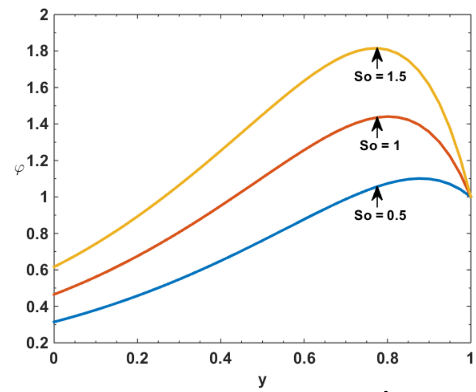

Figure 3. Particle concentration φ vs y for $\lambda = 5$, $Re = 2$, $Gr = .5$, $Gm = -.5$, $Pr = 0.71$, $Sc = .84$, $F = 1$, $M = 1$, $h_1 = 0.5$, $h_2 = 0.5$, $h_3 = 0.5$, $f = 0.2$, $\Lambda = 0.2$, $z = 0.0$, $t = 0.0$, $\varepsilon = 0.05$

Table 1. Shear stress due to main flow at $y = 0$ for $\lambda = 5$, $Gr = .5$, $Gm = -.5$, $Re = 2$, $Pr = 0.71$, $S = 1$, $M = 1$, $F = 1$, $h_1 = 0.5$, $h_2 = 0.5$, $h_3 = 0.5$, $f = 0.2$, $\Lambda = 0.2$, $z = 0.0$, $t = 0.0$, $\varepsilon = 0.05$

Sc	Re_x			$\tan\phi_x$	
	$So = 0.5$	$So = 1$	$So = 1.5$	$So = 0.5$	$So = 1$
0.5	13.4225	18.1286	22.8347	-0.4003	-0.4007
1	4.7319	7.4123	10.0927	-0.0201	-0.0178
1.5	3.0550	5.3350	7.6153	1.2386	1.2646

5. Conclusion

We extended the result of Guria [6] to study the effect of mass transfer and with slip condition on the three dimensional unsteady hydromagnetic couette flow of viscous incompressible fluid between two horizontal porous flat plates. The conclusions of the study are:

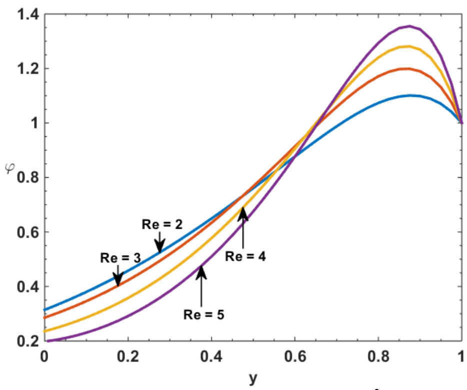

Figure 4. Particle concentration φ vs y for $\lambda = 5$, $Gr = .5$, $Gm = -.5$, $Pr = 0.71$, $Sc = .84$, $So = 0.5$, $S = 1$, $F = 1$, $M = 1$, $h_1 = 0.5$, $h_2 = 0.5$, $h_3 = 0.5$, $f = 0.2$, $\Lambda = 0.2$, $z = 0.0$, $t = 0.0$, $\varepsilon = 0.05$

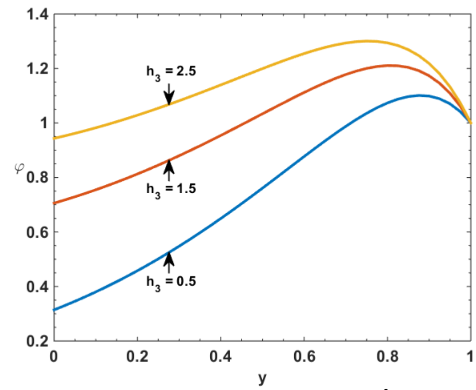

Figure 6. Particle concentration φ vs y for $\lambda = 5$, $Gr = .5$, $Gm = -.5$, $Re = 2$, $Pr = 0.71$, $Sc = .84$, $So = 0.5$, $S = 1$, $F = 1$, $M = 1$, $h_1 = 0.5$, $h_2 = 0.5$, $f = 0.2$, $\Lambda = 0.2$, $z = 0.0$, $t = 0.0$, $\varepsilon = 0.05$

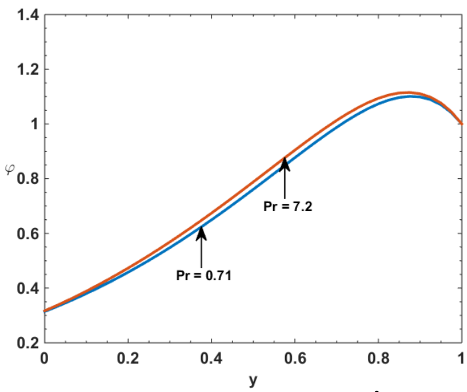

Figure 5. Particle concentration φ vs y for $\lambda = 5$, $Gr = .5$, $Gm = -.5$, $Re = 2$, $Sc = .84$, $So = 0.5$, $F = 1$, $M = 1$, $h_1 = 0.5$, $h_2 = 0.5$, $h_3 = 0.5$, $f = 0.2$, $\Lambda = 0.2$, $z = 0.0$, $t = 0.0$, $\varepsilon = 0.05$

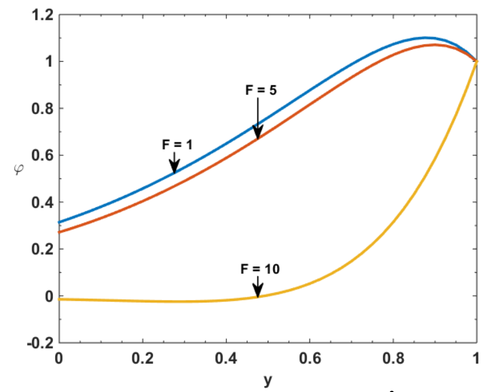

Figure 7. Particle concentration φ vs y for $\lambda = 5$, $Gr = .5$, $Gm = -.5$, $Re = 2$, $Pr = 0.71$, $Sc = .84$, $So = 0.5$, $S = 1$, $M = 1$, $h_1 = 0.5$, $h_2 = 0.5$, $h_3 = 0.5$, $f = 0.2$, $\Lambda = 0.2$, $z = 0.0$, $t = 0.0$, $\varepsilon = 0.05$

Table 2. Shear stress due to main flow at $y = 0$ for $\lambda = 5$, $Gr = .5$, $Re = 2$, $Pr = 0.71$, $Sc = 0.84$, $So = 1.5$, $S = 1$, $M = 1$, $F = 1$, $h_1 = 0.5$, $h_2 = 0.5$, $h_3 = 0.5$, $f = 0.2$, $\Lambda = 0.2$, $z = 0.0$, $t = 0.0$, $\varepsilon = 0.05$

Gm	Re_x	$\tan\phi_x$
-0.5	11.9139	-0.2193
0	0.0911	-0.1535
0.5	11.7321	-0.2203

Table 3. Sherwood number at $y = 0$ for $\lambda = 5$, $Gr = .5$, $Gm = -.5$, $Re = 2$, $Pr = 0.71$, $S = 1$, $M = 1$, $F = 1$, $h_1 = 0.5$, $h_2 = 0.5$, $h_3 = 0.5$, $f = 0.2$, $\Lambda = 0.2$, $z = 0.0$, $t = 0.0$, $\varepsilon = 0.05$

Sc	Re_C			$\tan\phi_C$	
	$So = 0.5$	$So = 1$	$So = 1.5$	$So = 0.5$	$So = 1$
0.5	0.3744	0.7614	1.1542	-68.7623	-5.8637
1	1.8319	3.7211	5.6106	0.6583	0.6389
1.5	0.7411	1.4992	2.2608	-0.7731	-0.6479

➢ Increasing the Schmidt number (Sc) and Soret number (So) increases the particle concentration in the fluid.

➢ Increasing the Soret number increases the main flow velocity for both fluid and particle phase with no effect on cross-flow velocity.

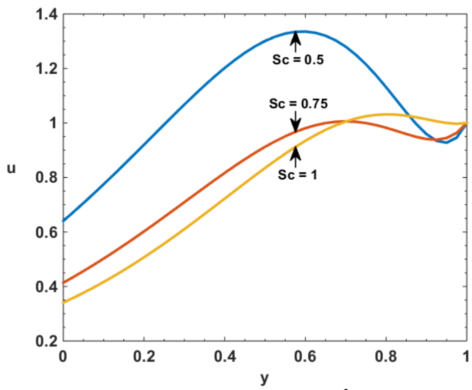

Figure 8. Main flow velocity u vs y for $\lambda = 5$, $Gr = .5$, $Gm = -.5$, $Re = 2$, $Pr = 0.71$, $So = 0.5$, $S = 1$, $M = 1$, $F = 1$, $h_1 = 0.5$, $h_2 = 0.5$, $h_3 = 0.5$, $f = 0.2$, $\Lambda = 0.2$, $z = 0.0$, $t = 0.0$, $\varepsilon = 0.05$

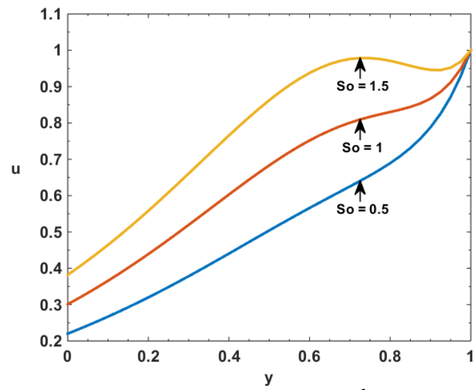

Figure 10. Main flow velocity u vs y for $\lambda = 5$, $Gr = .5$, $Gm = -.5$, $Re = 2$, $Pr = 0.71$, $Sc = 0.84$, $S = 1$, $M = 1$, $F = 1$, $h_1 = 0.5$, $h_2 = 0.5$, $h_3 = 0.5$, $f = 0.2$, $\Lambda = 0.2$, $z = 0.0$, $t = 0.0$, $\varepsilon = 0.05$

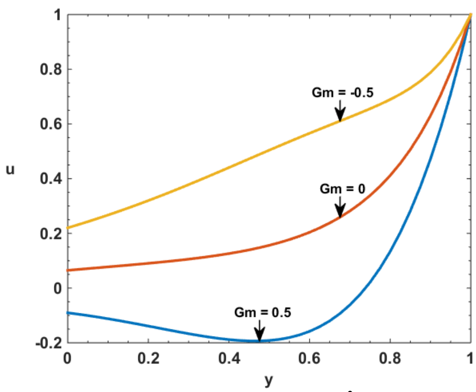

Figure 9. Main flow velocity u vs y for $\lambda = 5$, $Gr = .5$, $Gm = -.5$, $Re = 2$, $Pr = 0.71$, $So = 0.5$, $Sc = 0.84$, $S = 1$, $M = 1$, $F = 1$, $h_1 = 0.5$, $h_2 = 0.5$, $h_3 = 0.5$, $f = 0.2$, $\Lambda = 0.2$, $z = 0.0$, $t = 0.0$, $\varepsilon = 0.05$

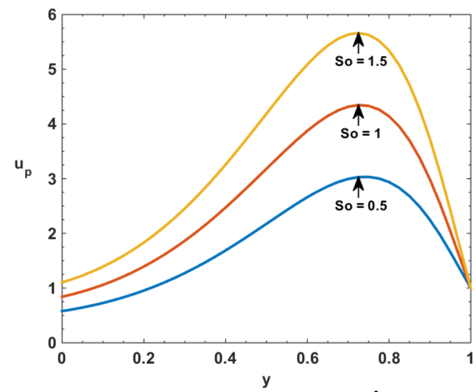

Figure 11. Main flow velocity u_p vs y for $\lambda = 5$, $Gr = .5$, $Gm = -.5$, $Re = 2$, $Pr = 0.71$, $Sc = 0.84$, $M = 1$, $F = 1$, $h_1 = 0.5$, $h_2 = 0.5$, $h_3 = 0.5$, $f = 0.2$, $\Lambda = 0.2$, $z = 0.0$, $t = 0.0$, $\varepsilon = 0.05$

Table 4. Sherwood number at $y = 0$ for $\lambda = 5$, $Gr = .5$, $Gm = -.5$, $Re = 2$, $Pr = 0.71$, $Sc = 0.84$, $So = 1.5$, $S = 1$, $M = 1$, $F = 1$, $h_1 = 0.5$, $h_2 = 0.5$, $h_3 = 0.5$, $f = 0.2$, $\Lambda = 0.2$, $z = 0.0$, $t = 0.0$, $\varepsilon = 0.05$

Sc	Re_C				$\tan\phi_C$
2	4.0758	5.2474	5.5394	3.1085	3.2574
3	6.7222	8.1581	8.5494	213.9872	-5.8403
4	5.9079	5.6431	5.6012	-10.9986	-2.3699
5	14.7582	13.5380	13.3314	-1.8125	-0.9572

- ➢ Increase in the Reynolds number (Re) results in a rise in the amplitude of oscillations in the particle concentration.
- ➢ Higher values of slip mass parameter imply a larger particle concentration.
- ➢ Increasing Schmidt number (Sc) decreases the amplitude of the shear stress and the tangent of phase shift.
- ➢ Increasing the Soret number (So) results in an increase in the amplitude of Sherwood number and the tangent of phase shift.
- ➢ Sherwood number increases with increasing mass slip parameter at lower Reynolds number and decreases with increasing mass slip parameter at higher Reynolds number.

Acknowledgment

The authors are deeply grateful to the anonymous referees and the editor for their careful reading and correction of some errors, which have greatly improved the quality of the paper.

References

[1] S. Ahmed, K. Kalita and A.J. Chamkha, Analytical and numerical solution of three-dimensional channel flow in presence of a sinusoidal fluid injection and a chemical reaction, *Ain Shams Engineering Journal*, 6 (2015) 691-701.

[2] T. Chinyoka, and O.D. Makinde, Analysis of transient Generalized Couette flow of a reactive variable viscosity third-grade liquid with asymmetric convective cooling, *Mathematical and Computer Modelling*, 54 (2011) 160-174.

[3] S.Das S, R.N. Jana and O.D. Makinde, Transient hydromagnetic reactive Couette flow and heat transfer in a rotating frame of reference, *Alexandria Engineering Journal*, 55 (2016) 635-644.

[4] E.R.G. Eckert, *Heat and Mass Transfer*, McGraw-Hill, New York, 1958.

[5] A. Govindarajan, V. Ramamurthy and K. Sundarammal, 3D Couette flow of dusty fluid with transpiration cooling, *Journal of Zhejiang University SCIENCE A*, 8 (2007) 313-322 .

[6] M. Guria, Effect of slip condition on vertical channel flow in the presence of radiation, International Journal of Applied Mechanics and Engineering, 21 (2016) 341-358.

[7] O.D. Makinde, and T. Chinyoka, Numerical study of unsteady hydromagnetic Generalized Couette flow of a reactive third-grade fluid with asymmetric convective cooling, *Computer and Mathematics with Applications*, 12 (2011) 1167-1179.

[8] S.N. Sahoo, Heat and Mass Transfer Effect on MHD Flow of a Viscoelastic Fluid through a Porous Medium Bounded by an Oscillating Porous Plate in Slip Flow Regime, *International Journal of Chemical Engineering*, 15 (2013) 65-79.

[9] R. Sivaraj and R.B. Kumar, Chemically reacting dusty viscoelastic fluid flow in an irregular channel with convective boundary, *Ain Shams Engineering Journal*, 4 (2013) 93-101.

[10] T. Saravanakumar, V.J. Nirmala, R. Raja, J. Cao and G. Lu, Finite-time reliable dissipative control of neutral-type switched artificial neural networks with non-linear fault inputs and randomly occurring uncertainties, *Asian Journal of Control*, 22 (2020) 2487-2499.

[11] V. J. Nirmala, T. Saravanakumar and Q. Zhu, Dissipative criteria for Takagi-Sugeno fuzzy Markovian jumping neural networks with impulsive perturbations using delay partitioning approach, *Advances in Difference Equations*, 2019 (2019) 1-20.

[12] Q. Zhu, T. Saravanakumar, S. Gomathi and S. Marshal Anthoni, Dissipative criteria for Takagi-Sugeno fuzzy Markovian jumping neural networks with impulsive perturbations using delay partitioning approach, *IEEE Access*, 7 (2019) 90289-90303.

[13] T. Saravanakumar, S. Marshal Anthoni and Q. Zhu, Resilient extended dissipative control for Markovian jump systems with partially known transition probabilities under actuator saturation, *Journal of the Franklin Institute*, 357 (2020) 6197-6227.

[14] T. Saravanakumar, N.H.Muoi and Q. Zhu, Finite-time sampled-data control of switched stochastic model with non-deterministic actuator faults and saturation nonlinearity, *Journal of the Franklin Institute*, 357 (2020) 13637-13665.

[15] T. Poongodi, T. Saravanakumar and Q. Zhu, Extended dissipative control for markovian jump time-delayed systems with bounded disturbances, *Mathematical Problems in Engineering*, 2020 (2020) 1-15.

⋆⋆⋆⋆⋆⋆⋆⋆⋆
ISSN(P):2319 − 3786
Malaya Journal of Matematik
ISSN(O):2321 − 5666
⋆⋆⋆⋆⋆⋆⋆⋆⋆